Histol Histopathol (2023) 38: 303-316

http://www.hh.um.es

Histology and Histopathology
From Cell Biology to Tissue Engineering

ORIGINAL ARTICLE **Open Access**

Circ_0031242 regulates the functional properties of hepatocellular carcinoma cells through the miR-944/MAD2L1 axis

Jianwei Lin[1], Zenghai Lin[1], Yaqiong Hua[2] and Yan Chen[2]

[1]Department of General Surgery, The First Affiliated Hospital of Shantou University Medical College, Shantou and
[2]Department of Medicine, Shenzhen Letu Biotechnology Co., Ltd., Guangdong, China

Summary. Background. Circular RNAs (circRNAs) possess key functions in the pathogenesis of hepatocellular carcinoma (HCC). Nonetheless, the actions of individual circRNAs in HCC remain undefined.

Methods. circ_0031242, miR-944, and MAD2L1 expression were quantified by qRT-PCR. Transwell assay was utilized to examine cell invasion and migration. Glucose consumption and lactate production were measured to assess the impact on glycolysis. The relationships among circ_0031242, MAD2L1, and miR-944 were examined via luciferase reporter assay.

Results. circ_0031242 was notably augmented in HCC. Loss of function of circ_0031242 hindered cell proliferation, invasion, migration, glycolysis, and promoted apoptosis, as well as impeding HCC tumor growth. circ_0031242 directly targeted miR-944. Inhibition of miR-944 counteracted the effects of si-circ_0031242 on HCC cells. Additionally, miR-944 was proved to directly target MAD2L1 in HCC cells. Moreover, the promotion of MAD2L1 was able to rescue the inhibition of high miR-944 expression on HCC cell progression. Meanwhile, circ_0031242 involved the post-transcriptional modulation of MAD2L1 through miR-944.

Conclusion. This study suggested that circ_0031242 regulated tumor cell progression and tumor growth through the miR-944/MAD2L1 axis in HCC.

Key words: circ_0031242, miR-944, MAD2L1, HCC, Cell progression, Glycolysis

Corresponding Author: Zenghai Lin, MM, Department of General Surgery, The First Affiliated Hospital of Shantou University Medical College, No. 57, Changping Road, Shantou City, Guangdong Province, 515041, China. e-mail: jwlin3@126.com

DOI: 10.14670/HH-18-519

Introduction

Hepatocellular carcinoma (HCC) remains one of the most prevalent cancers globally (Shen et al., 2018; Kaibori et al., 2019). Despite the continuous development of therapeutic methods, their therapeutic effects remain unsatisfactory. Therefore, understanding the pathogenesis of HCC and finding new effective methods are of great significance for increasing the cure rate and improving prognosis.

Circular RNAs (circRNAs) are naturally occurring RNAs with a closed covalent circular structure (Qiu et al., 2019). Understanding and exploration of circRNA have been deepening. The report of Xiong et al. revealed that circRNAs have miRNA binding sites and can work as a ceRNA to form a circRNA-miRNA axis in HCC Xiong et al., 2018). Up to now, circRNAs have established important regulatory roles in various cancers, including HCC (Hsiao et al., 2017; Yao et al., 2017; Zhang et al., 2017, 2018; Qu et al., 2019). For instance, circ_0025202 was expressed in low levels in breast cancer cells and performed key effects on physiological processes such as cell metastasis and sensitivity to tamoxifen by affecting the miR-182-5p/FOXO3a axis (Sang et al., 2019). Abnormal expression of circRNA has been found in HCC and participates in the oncogenesis of HCC, which has great application value for disease prediction and therapeutic targets (Qin et al., 2016; Wang et al., 2019a,b; Wei et al., 2020a,b). For instance, circ_001955 was enhanced in HCC and closely related to tumor development (Yao et al., 2019; Ding et al., 2020b). However, there are many circRNAs whose critical actions in HCC have not been identified.

Here, we collected HCC samples from clinical patients and observed that circ_0031242 is elevated in HCC tissues, implying that circ_003124 was related to the pathogenesis of HCC. However, the related functions and the detailed mechanisms of circ_003124 remain

unclear.

Materials and methods

Human subject study

We obtained HCC tissues and their adjacent nontumor tissues (ANT) from surgical resection of 32 patients at The First Affiliated Hospital of Shantou University Medical College. This research was conducted with approval from the Ethics Committee of The First Affiliated Hospital of Shantou University Medical College. We received written consent from the HCC patients (who underwent surgical resection) and their families. All collected tissues were stored in a refrigerator at -80°C for subsequent experiments.

Cell lines

HCC cells (SNU-387, Huh-7, and HCCLM3) and THLE-2 liver cells were provided by American Type Culture Collection. Transfected cells and non-transfected cells were propagated in RPMI-1640 medium (Life Technologies, Scotland, UK), which included 10% FBS (Life Technologies).

SiRNA and oligonucleotide transfection

Si-circ_0031242, oe-circ_0031242, pcDNA-MAD2L1, and the matched control mocks (si-NC, oe-NC, and pcDNA-con), miR-944 inhibitors and mimics were from Generaybiotech (Beijing, China). Lipofectamine 2000 reagent (Life Technologies) was utilized to introduce siRNA and miRNA mimics and inhibitors into Huh-7 and SNU-387 cell lines as per the accompanying recommendations.

qRT-PCR

For circ_0031242 and mRNA, the TaKaRa PrimeScript RT Master was applied to convert cDNA from total RNA treated without or with RNase R (Geneseed, Guangzhou, China); qRT-PCR was carried out to detect circ_0031242 and MAD2L1 using SYBR Green mix (TaKaRa). miR_944 expression was detected using the TaqMan MiRNA RT kit and TaqMan MiRNA assay kit, from Thermo Fisher Scientific (Runcorn, UK). Each sample was replicated three times. circ_0031242, miR-944, and MAD2L1 expression were determined via the $2^{-\Delta\Delta Ct}$ method, normalizing to GAPDH or U6 internal control gene. The primer (5'-3') of U6: forward, CTCGCTTCGGCAGCACATA; reverse, CGAATTTGC GTGTCATCCT. The primer (5'-3') of MAD2L1: forward, ACTTTTGAAACGCTTGGCGG; reverse, GAGAAGAACTCGGCCACGAT. The primer (5'-3') of miR-944: forward, GCCGAGAAATTATTGTACATC GG; reverse, CTCAACTGGTGTCGTGGA. The primer (5'-3') of GAPDH: forward, AAGGCTGTGGGCAAGG

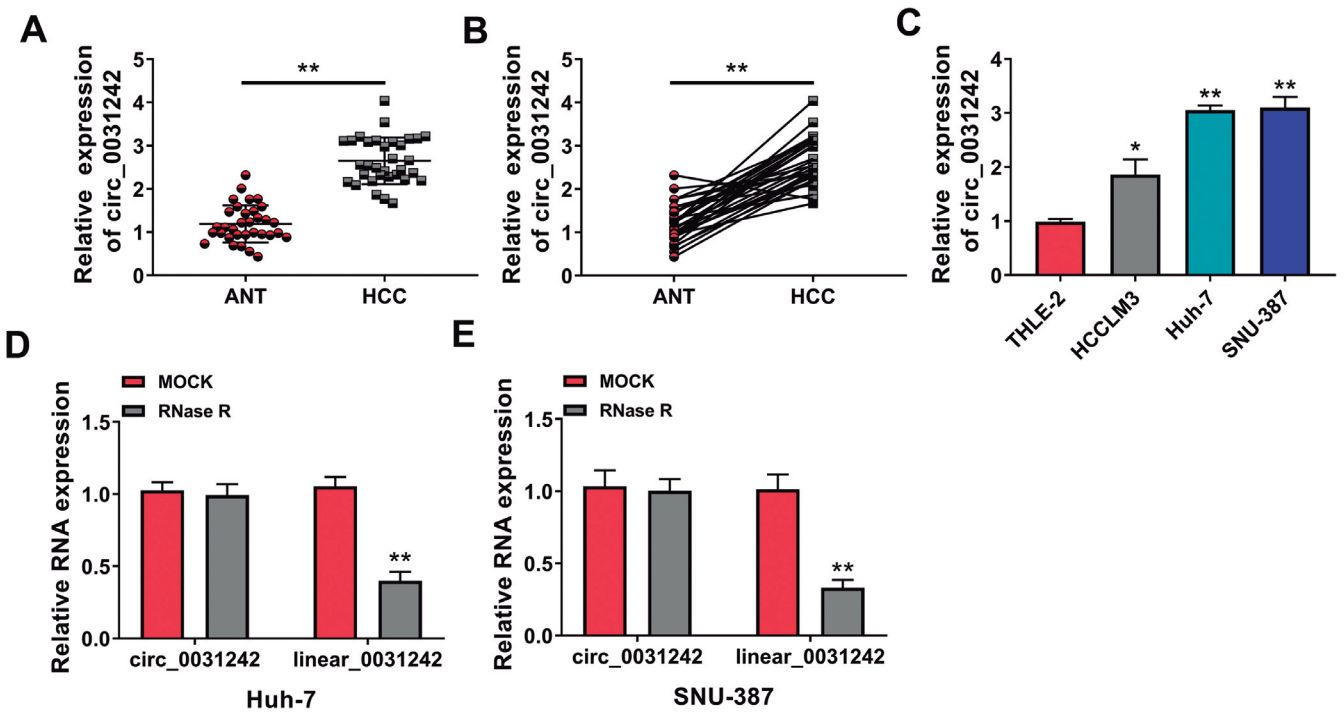

Fig. 1 Circ_0031242 was notably upregulated in HCC. **A and B.** Circ_0031242 level in HCC tissues compared with ANT tissues. **C.** Circ_0031242 expression was evaluated in HCCLM3, Huh-7 and SNU-387 cells compared with THLE-2 cells. **D and E.** The expression of circ_0031242 and linear mRNA was assessed after RNase R treatment. *p<0.05, **p<0.01.

TCATC; reverse, GCGTCAAAGGTGGAGGAGTGG. The primer (5'-3') of circ_0031242: forward, TGAACGGATTTTCAGCCTTT; reverse, ATGGCTG AAGGTGAAACAGG.

Western blot

Total proteins were separated through SDS–polyacrylamide gel electrophoresis with 90V for 1.5h and blotted onto PVDF membranes at 90mA (Millipore, USA). For immunoblotting, we used primary antibodies including anti-MAD2L1, anti-HK2, and anti-GAPDH, anti-Bax, anti-Bcl-2, and secondary antibody (anti-HRP-conjugated), from Abcam. Each experiment was carried out in triplicate.

Dual luciferase report assay

The MAD2L1 3'-UTR or circ_0031242 containing a predicted binding site or a mutated site sequence for miR-944 were cloned downstream of pmirGLO vector (Promega, Tokyo, Japan), named MAD2L1 WT, MAD2L1 MUT, circ_0031242 WT, circ_0031242 MUT, respectively. We transfected the cells using Lipofectamine 2000 with MAD2L1 WT (MAD2L1 MUT) or circ_0031242 WT (circ_0031242 MUT) and miRNA mimic. At 48 h after transfection, we determined luciferase activity with the Promega assay system.

Flow cytometry

Analysis was assessed using the Annexin V-FITC/PI Kit as described by the manufacturers (Beyotime, Beijing, China). We employed the FACSCalibur for the measurement of the apoptosis rate.

Colony formation and CCK-8 assays

~100 transfected SNU-367 and Huh-7 cells were added in 6-well dishes, followed by incubation for 10

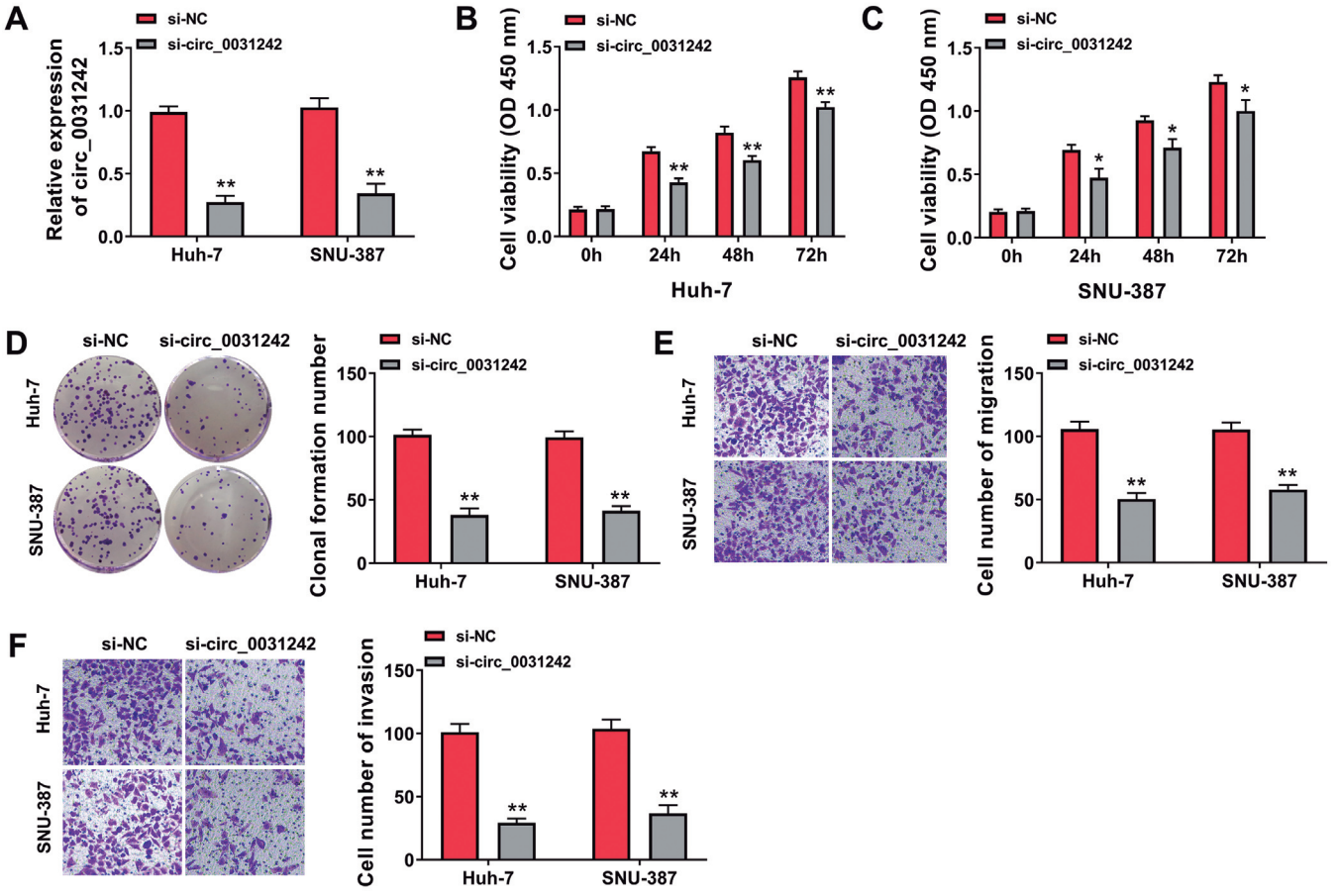

Fig. 2 Inhibition of circ_0031242 affected HCC cell proliferation, invasion, and migration. **A.** Circ_0031242 expression was gauged in si-NC- or si-circ_0031242-transfected Huh-7 and SNU-387 cells. CCK-8 assay **(B and C)** and colony formation assay **(D)** were applied for the assessment of the proliferation of transfected cells. **E and F.** Transwell migration and invasion assay was employed for the evaluation of migrative and invasive abilities of transfected cells. *p<0.05, **p<0.01.

days at 37°C. After crystal violet staining, colonies (≥ 50 cells) were counted.

Approximately 2000 transfected SNU-367 and Huh-7 cells were seeded in 96-well dishes. Cell proliferation assays were detected at the appropriate assay period with the CCK-8 solution (Dojindo, Rockville, MD, USA). Cell viability was measured by absorbance (450 nm). The experiment was done 3 times.

Transwell assay

Transfected SNU-367 and Huh-7 cells in RPMI-1640 medium were plated in Transwell insert coated without or with Matrigel (Millipore, Shanghai, China). The inserts were placed in 10%FBS RPMI-1640 media. The invasive or migrated cells were scored 24h later with a light microscope to analyze the capacity of migration and invasion after crystal violet staining.

Evaluation of lactate production and glucose consumption

We employed the Human Lactate Assay Kit and Glucose Assay Kit to perform these assays as described by the manufacturers (BioVision, Milpitas, CA, USA). Each sample was replicated three times.

Animal experiment

With the protocol approved by the Animal Research Committee of The First Affiliated Hospital of Shantou University Medical College, we injected subcutaneously stably transfected Huh-7 cells (4×10^6) into BALB/c female nude mice (five-week-old). Tumor volume was periodically calculated (formula: volume = width2 × length/2). 4 weeks later, we weighed and collected xenografts from killed mice to detect circ_0031242, miR-944, and MAD2L1 levels.

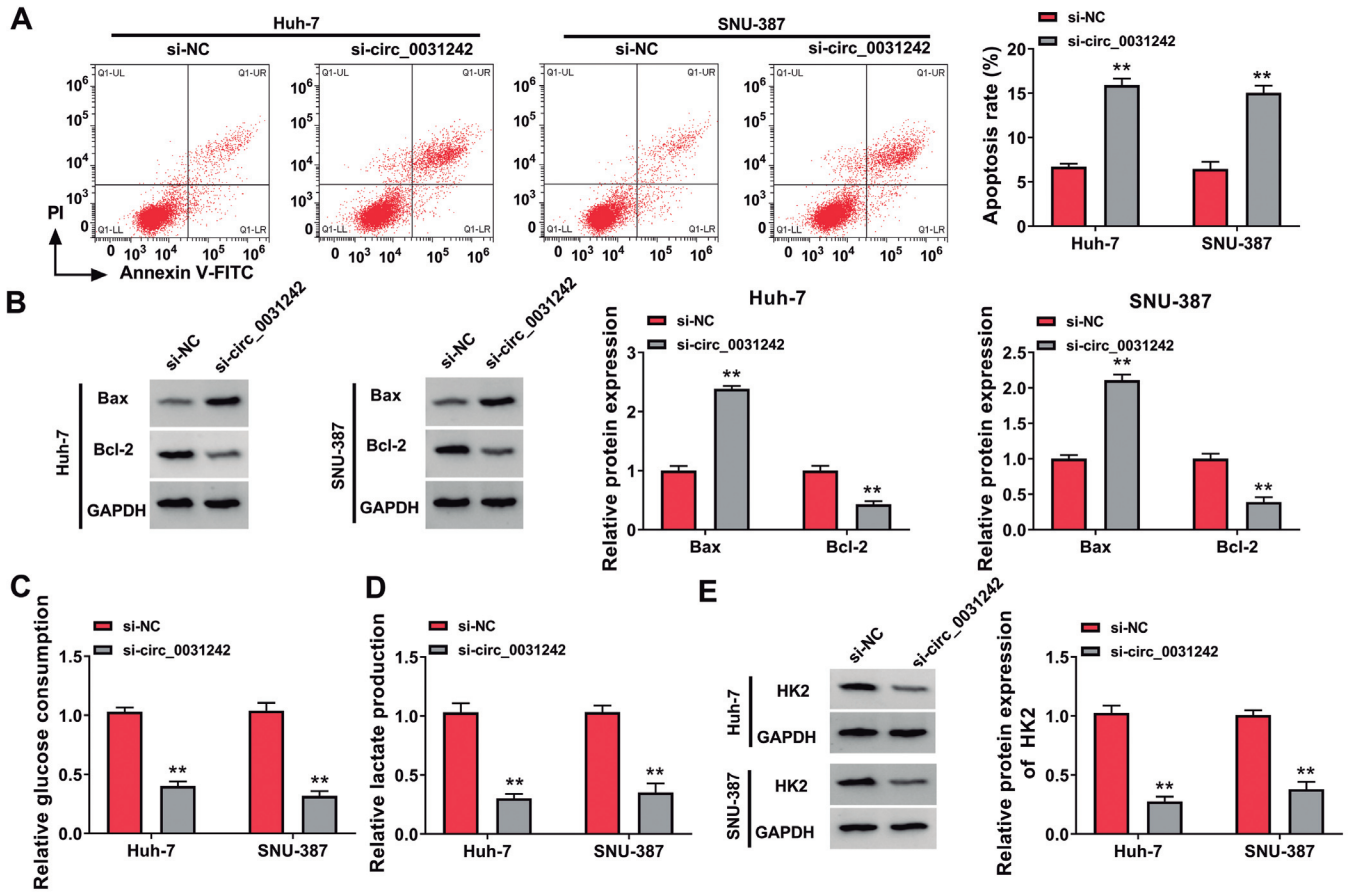

Fig. 3. Inhibition of circ_0031242 affected HCC cell apoptosis and glycolysis. **A.** Apoptosis of si-circ_0031242-transfected or si-NC-introduced Huh-7 and SNU-387 cells was checked by flow cytometry. **B.** Western blot showing Bax and Bcl-2 expression in si-circ_0031242-transfected or si-NC-introduced Huh-7 and SNU-387 cells. **C and D.** Glucose consumption and lactate production in si-circ_0031242-transfected or si-NC-introduced Huh-7 and SNU-387 cells. **E.** Western blot was applied to assess HK2 level in si-circ_0031242-transfected or si-NC-introduced Huh-7 and SNU-387 cells. $^{**}p<0.01$.

Immunohistochemistry assay (IHC)

The tumor tissues of the mice were collected, cut into pieces with a thickness of no more than 5 mm, and fixed with 10% neutral formalin. Then, a DAKO EnVisionTM system (Dako, Glostrup, Denmark) was used for IHC following the instructions. The primary antibody used was Ki67 (Abcam). We observed and counted the number of Ki67 positive cells microscopically.

Statistical analysis

Each assay was conducted on three or more biological replicates. Two-tailed student's *t*-test (for two groups) or one-way ANOVA test (three or more groups)

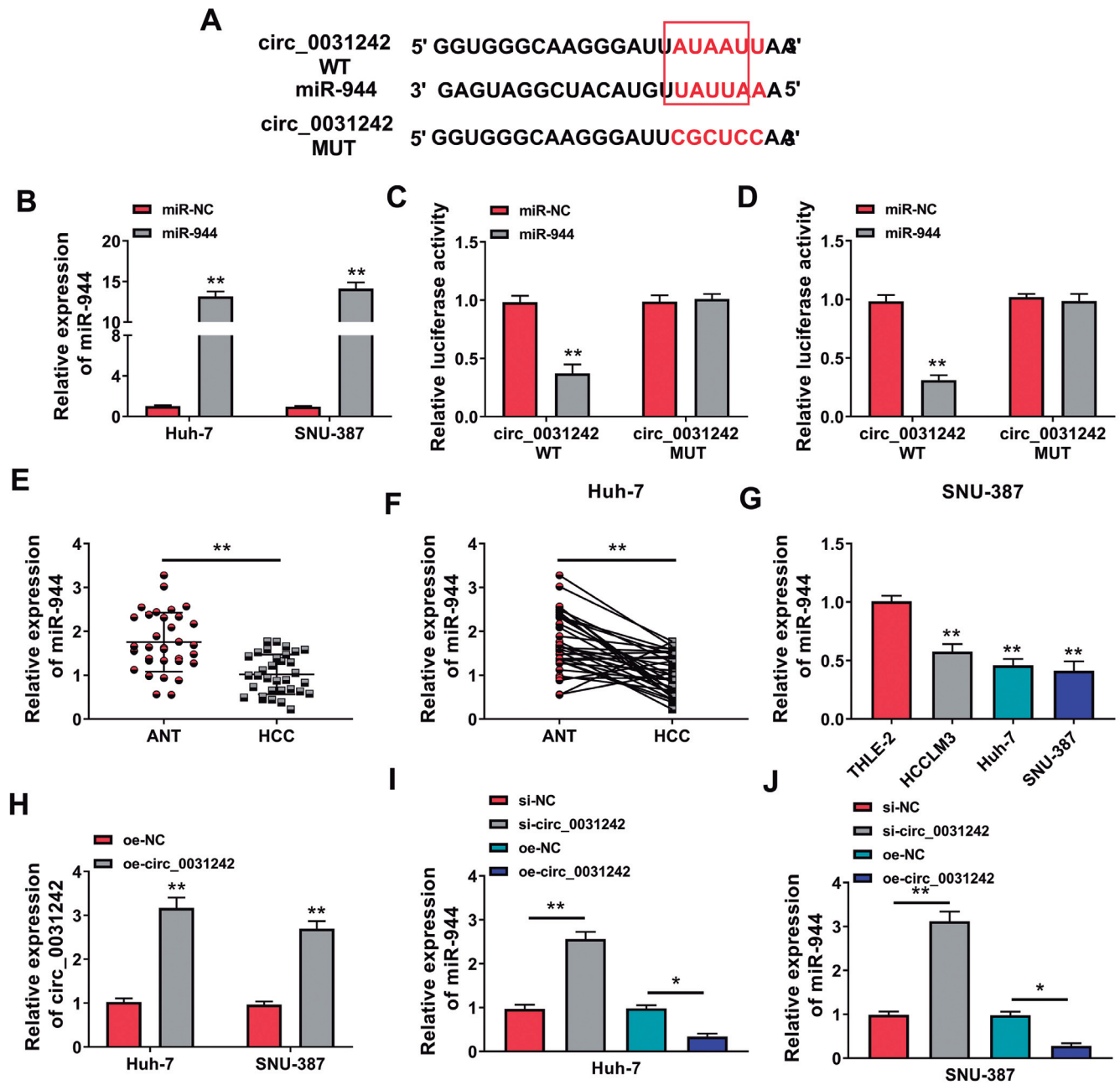

Fig. 4. Circ_0031242 targeted miR-944. **A.** The interaction between circ_0031242 and miR-944 was predicted by starBase v2.0. **B.** miR-944 expression in miR-944-transfected or miR-NC-introduced SNU-387 and Huh-7 cells. **C and D.** The luciferase activity of Huh-7 and SNU-387 cells. **E and F.** miR-944 expression in HCC tissues compared to ANT tissues. (G) miR-944 expression in HCCLM3, Huh-7 and SNU-387 cells compared to THLE-2 cells. **H.** Circ_0031242 expression in oe-circ_0031242-transfected or oe-NC-introduced Huh-7 and SNU-387 cells. **I and J.** miR-944 level was gauged in SNU-387 and Huh-7 cells introduced by si-circ_0031242, si-NC, oe-NC or oe-circ_0031242. **p*<0.05, ***p*<0.01.

were employed to analyze the statistical significance. p values < 0.05 were defined as significant.

Results

Circ_0031242 was upregulated in HCC

In contrast to the adjacent nontumor tissues, circ_0031242 was significantly promoted in HCC tissues (Fig. 1A,B). Moreover, circ_0031242 in HCC cell lines (HCCLM3, Hub-7, SNU-387) was markedly enhanced compared with the normal THLE-2 cell line (Fig. 1C). RNase R experiment results showed that circ_0031242 was more stable than linear_0031242 in SNU-387 and Huh-7 cells (Fig. 1D,E).

Inhibition of circ_0031242 affected HCC cell proliferation, invasion, migration, apoptosis, and glycolysis

qRT-PCR results showed that the expression of circ_0031242 was remarkably suppressed in the si-circ_0031242 group compared with the si-NC group (Fig. 2A). CCK-8 assays showed that cell viability of the si-circ_0031242 group was significantly reduced compared with the si-NC group (Fig. 2B,C). Similarly, the number of cell colonies of the si-circ_0031242 group was significantly reduced (Fig. 2D). Moreover, transwell assay verified the impact of circ_0031242 on cell metastasis. Cell migration and invasion were significantly suppressed by circ_0031242 depletion (Fig. 2E,F). Conversely, knockdown of circ_003124 induced

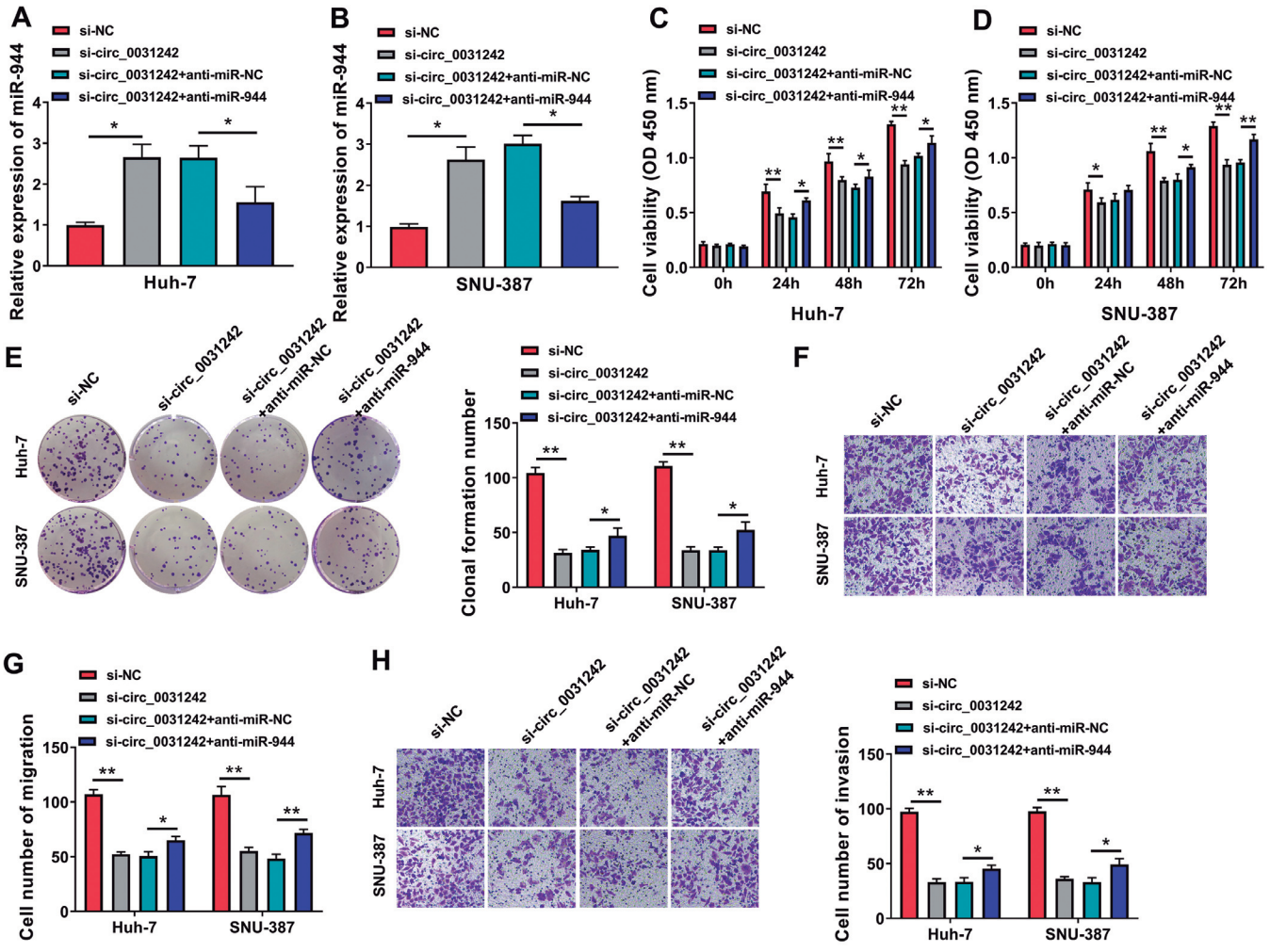

Fig. 5. Down-expression of miR-944 was able to reverse the effects of si-circ_0031242 on cell proliferation, invasion, and migration. **A and B.** MiR-944 level in Huh-7 and SNU-387 cells introduced by si-circ_0031242+anti-miR-944, si-circ_0031242+anti-miR-NC, si-circ_0031242 or si-NC. CCK-8 assay **(C and D)** and colony formation assay **(E)** were employed for the determination of proliferation of transfected cells. **F-H.** Transwell migration and invasion assays were applied for the measurement of migration and invasion of transfected cells. *p<0.05, **p<0.01.

the apoptosis of Huh-7 and SNU-387 cells (Fig. 3A), increased Bax protein and inhibited Bcl-2 protein in the two HCC cell lines (Fig. 3B). In addition, the glucose consumption, lactate production, and HK2 protein expression were significantly decreased by circ_0031242 depletion (Fig. 3C-E), implying that suppression of circ_0031242 also decreased the glycolysis of Huh-7 and SNU-387 cells.

Circ_0031242 sponged miR-944 in HCC cells

To further understand whether circ_0031242 participated in HCC by working as a ceRNA, we used starbase software to predict the miRNA-binding sites to circ_0031242 and found that miR-944 was a potential target miRNA of circ_0031242 (Fig. 4A). We then used the dual luciferase reporter assay to prove the possibility. The miR-944 overexpression efficacy of the miR-944 mimic was validated by qRT-PCR (Fig. 4B). Elevation of miR-944 dramatically reduced the luciferase activity of circ_0031242 WT, but did not reduce the reporter gene expression of circ_0031242 MUT (Fig. 4C,D). Intriguingly, miR-944 expression was at low levels in HCC tissues, SUN-387 and Huh-7 HCC cells (Fig. 4E-G). Moreover, overexpression of circ_0031242 by oe-circ_0031242 (Fig. 4H) significantly inhibited the level of miR-944, while low circ_0031242 level significantly induced miR-944 expression (Fig. 4I,J).

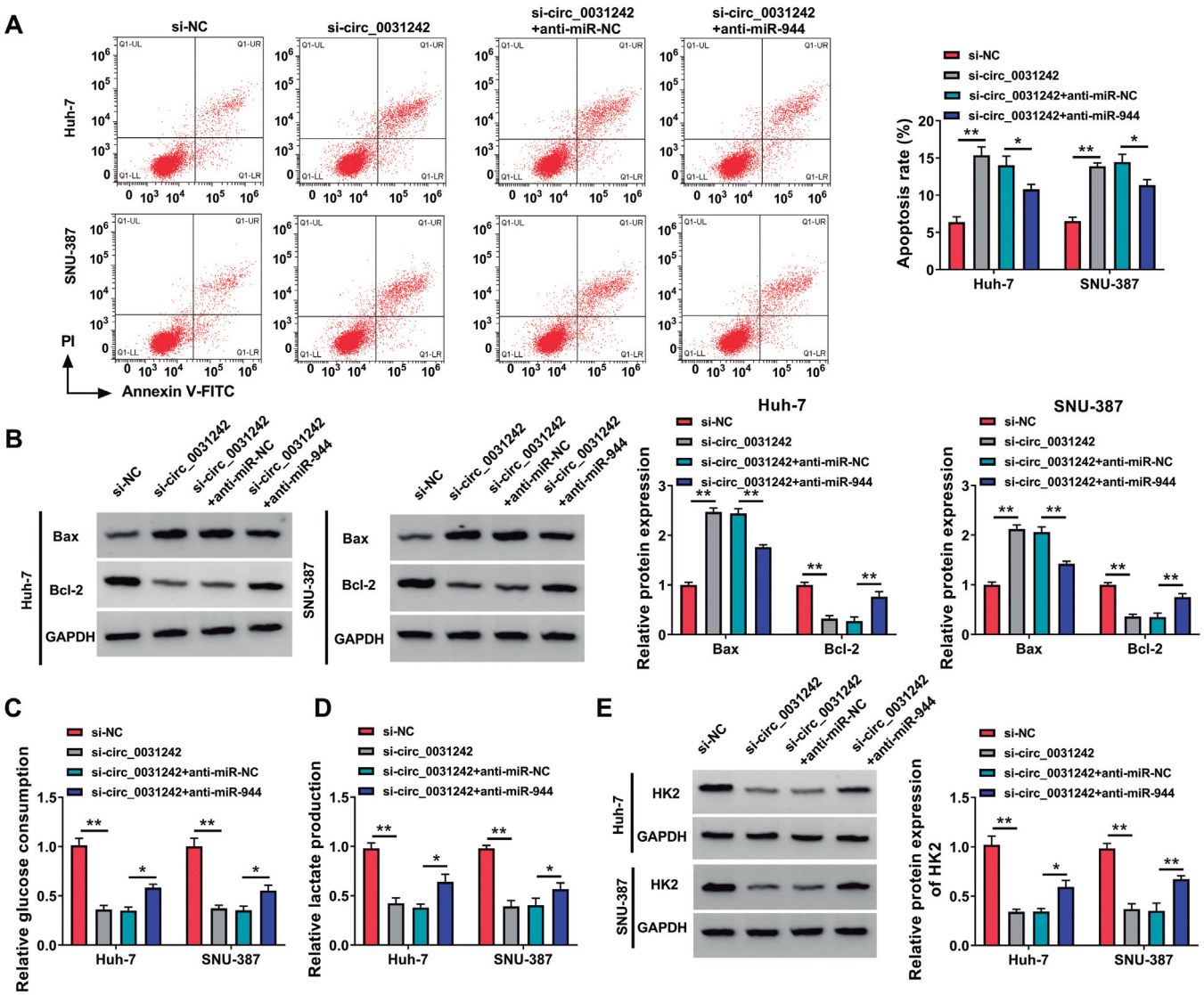

Fig. 6. Down-expression of miR-944 reversed the effects of si-circ_0031242 on cell apoptosis and glycolysis. **A.** Apoptosis of transfected cells by flow cytometry. Bax and Bcl-2 protein expression **(B)**, glucose consumption **(C)**, lactate production **(D)** and HK expression **(E)** in Huh-7 and SNU-387 cells introduced by si-circ_0031242+anti-miR-944, si-circ_0031242+anti-miR-NC, si-NC, or si-circ_0031242. *p<0.05, **p<0.01.

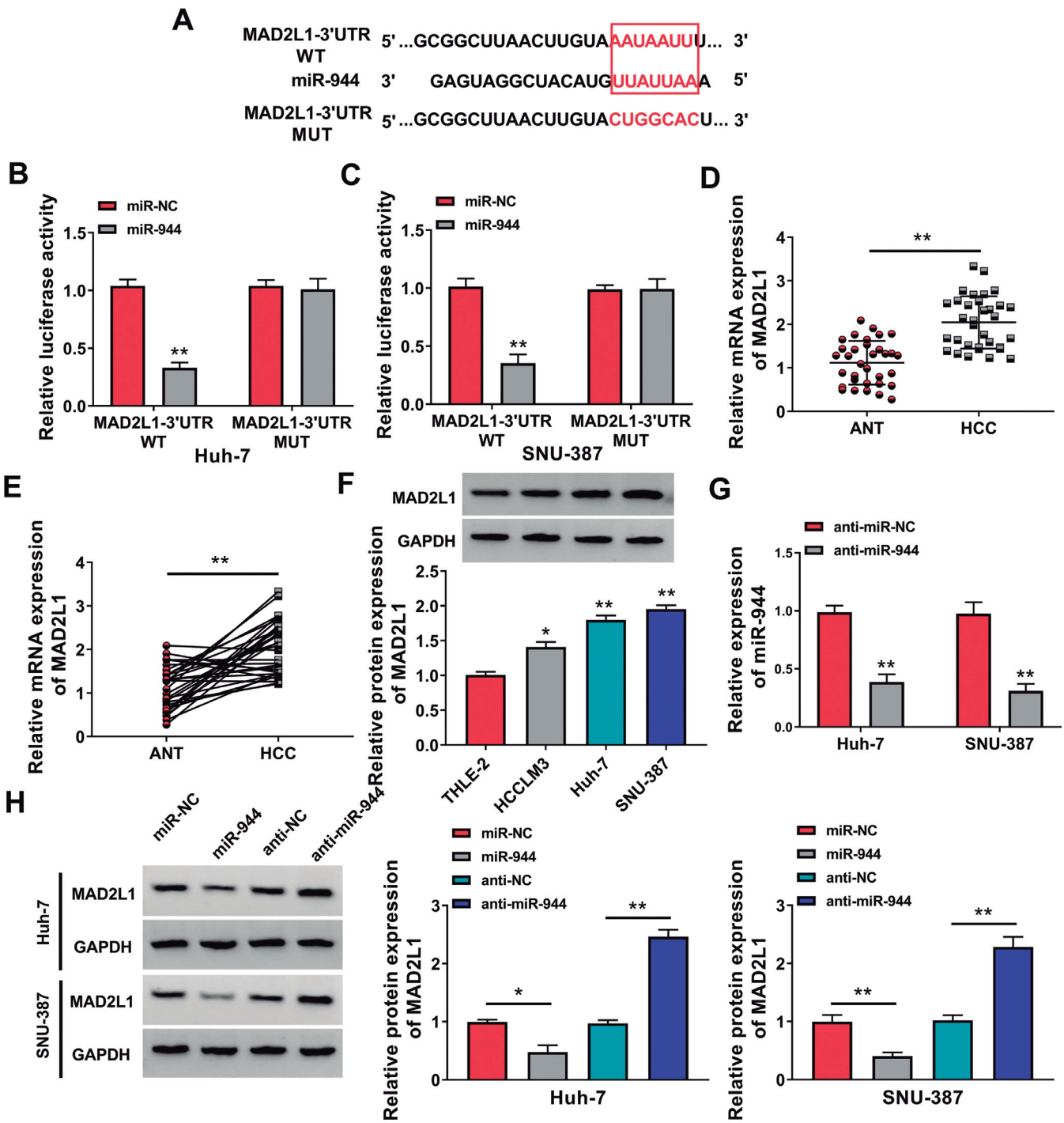

Fig. 7. MiR-944 targeted MAD2L1. **A.** The relationship between MAD2L1 and miR-944 was predicted by TargetScan. **B and C.** Dual-luciferase assays of SNU-387 and Huh-7 cells. **D and E.** MAD2L1 expression in HCC tissues compared to ANT tissues. **F.** The MAD2L1 protein level in HCCLM3, Huh-7 and SNU-387 cells compared to THLE-2 cells. **G.** MAD2L1 expression in anti-miR-NC- or anti-miR-944-transfected Huh-7 and SNU-387 cells. **H.** MAD2L1 expression in Huh-7 and SNU-387 cells introduced by anti-miR-944, anti-NC, miR-944 or miR-NC. *p<0.05, **p<0.01.

Down-expression of miR-944 reversed the effects of si-circ_0031242 on HCC cells

To further clarify the function of the relationship of miR-944 and circ_0031242 in HCC, we transfected si-circ_0031242+anti-miR-NC or si-circ_0031242+anti-miR-944 into Huh-7 and SUN-387 cells. As shown in Fig. 5A,B, transfection of anti-miR-944 reduced si-circ_0031242-induced elevation of miR-944 of Huh-7 and SUN-387 cells. The results of CCK-8 assay showed that knockdown of circ_0031242 reduced cell viability, which was enhanced by downregulation of miR-944 (Fig. 5C,D). Colony formation assay proved that low miR-944 expression could eliminate the inhibitory impact of circ_0031242 depletion on colony formation ability (Fig. 5E). Also, si-circ_0031242 transfection inhibited cell migration and invasion, which were abated by miR-944 reduction in Huh-7 and SUN-387 cells (Fig. 5F-H). Meanwhile, miR-944 reduction inhibited the apoptosis of SUN-387 and Huh-7 cells, which was induced by si-circ_0031242 (Fig. 6A,B). Additionally, miR-944 reduction markedly abolished the repression of si-circ_0031242 on glucose consumption, lactate production and HK2 protein level (Fig. 6C-E). These results indicated that circ_0031242 affected cell functional behaviors through binding to miR-944.

miR-944 targeted MAD2L1

Next, we predicted the target genes of miR-944 by TargetScan and found that MAD2L1 contained a putative complementary sequence for miR-944 (Fig. 7A). To ascertain this, we tested the predicted miR-944 binding sites within MAD2L1 3'UTR for their reactivity to miR-944 overexpression in dual-luciferase assays with or without mutation in the seed sequence. MAD2L1

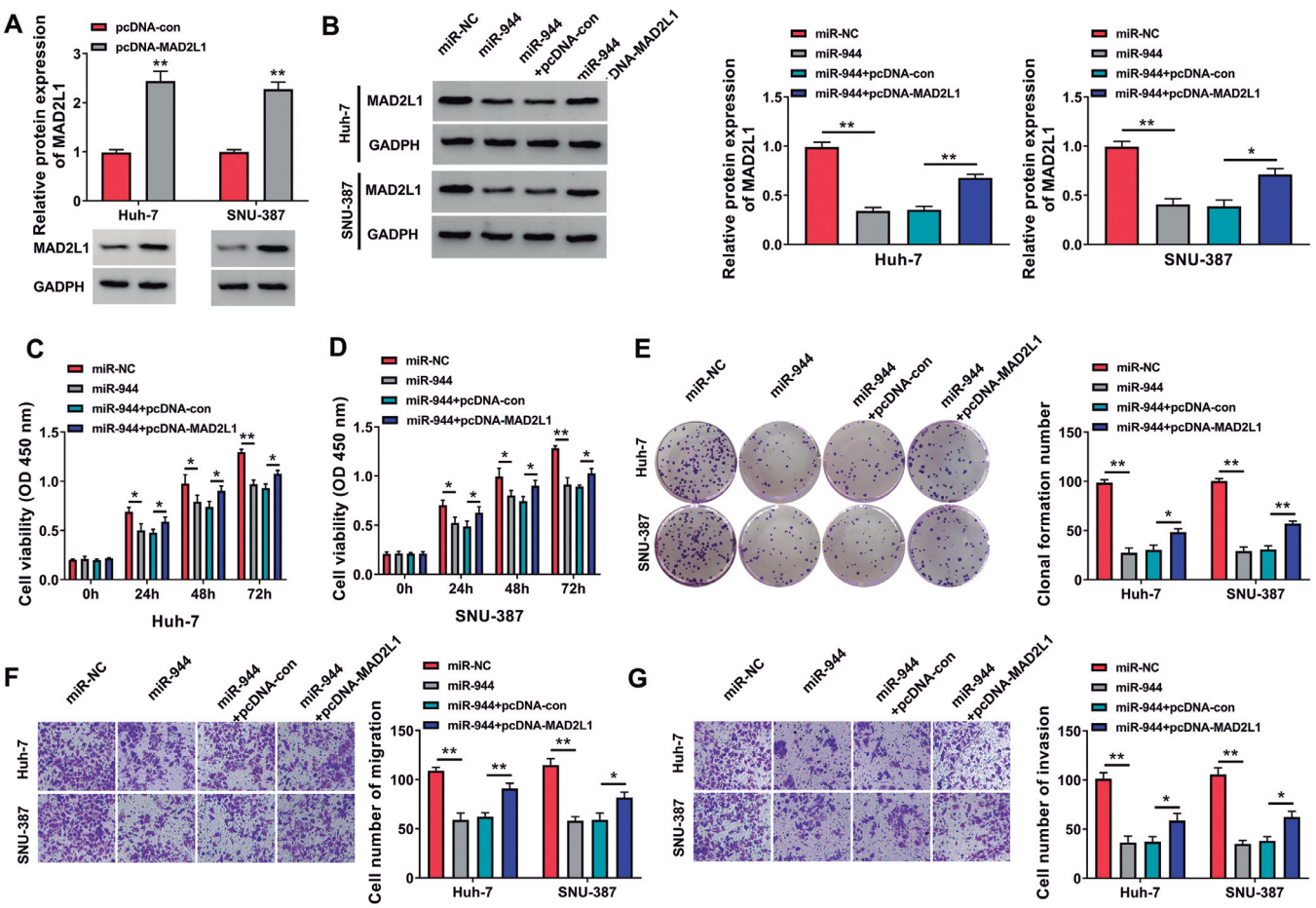

Fig. 8. Overexpression of MAD2L1 rescued the suppression of high miR-944 expression on HCC cell progression. **A.** MAD2L1 protein expression in pcDNA-MAD2L1-transfected or pcDNA-con-introduced SNU-387 and Huh-7 cells. **B.** MAD2L1 protein expression in SNU-387 and Huh-7 cells introduced by miR-944+pcDNA-MAD2L1, miR-944+pcDNA-con, miR-944 or miR-NC. MTT assay **(C and D)** and colony formation assay **(E)** were applied to the determination of proliferation of transfected cells. **F and G.** Transwell migration and invasion assays were employed for the assessment of migration and invasive abilities of transfected cells. *$p<0.05$, **$p<0.01$.

exhibited reactivity to miR-944 overexpression and showed a striking rescue after mutation in the predicted miR-944 binding sequence (Fig. 7B,C). In addition, MAD2L1 expression was highly elevated in HCC tissues, Huh-7 and SUN-387 HCC cells (Fig. 7D-F). As shown in Fig. 7G, anti-miR-944 transfection inhibited miR-944 expression in Huh-7 and SUN-387 cells. Moreover, MAD2L1 expression was inhibited by overexpression of miR-944, and conversely augmented by miR-944 inhibition in Huh-7 and SUN-387 cells (Fig. 7H). Thus, miR-944 targeted MAD2L1 in HCC cells.

Overexpression of MAD2L1 abolished the impact of high miR-944 expression on HCC cells

In order to explore the function of the relationship between miR-944 and MAD2L1, we upregulated MAD2L1 in SNU-387 and Huh-7 cells expressing miR-944. MAD2L1 expression was remarkably elevated by pcDAN-MAD2L1 transfection compared with the pcDNA-con control (Fig. 8A). By contrast, pcDNA-MAD2L1 transfection notably reversed miR-944 overexpression-caused repression of MAD2L1

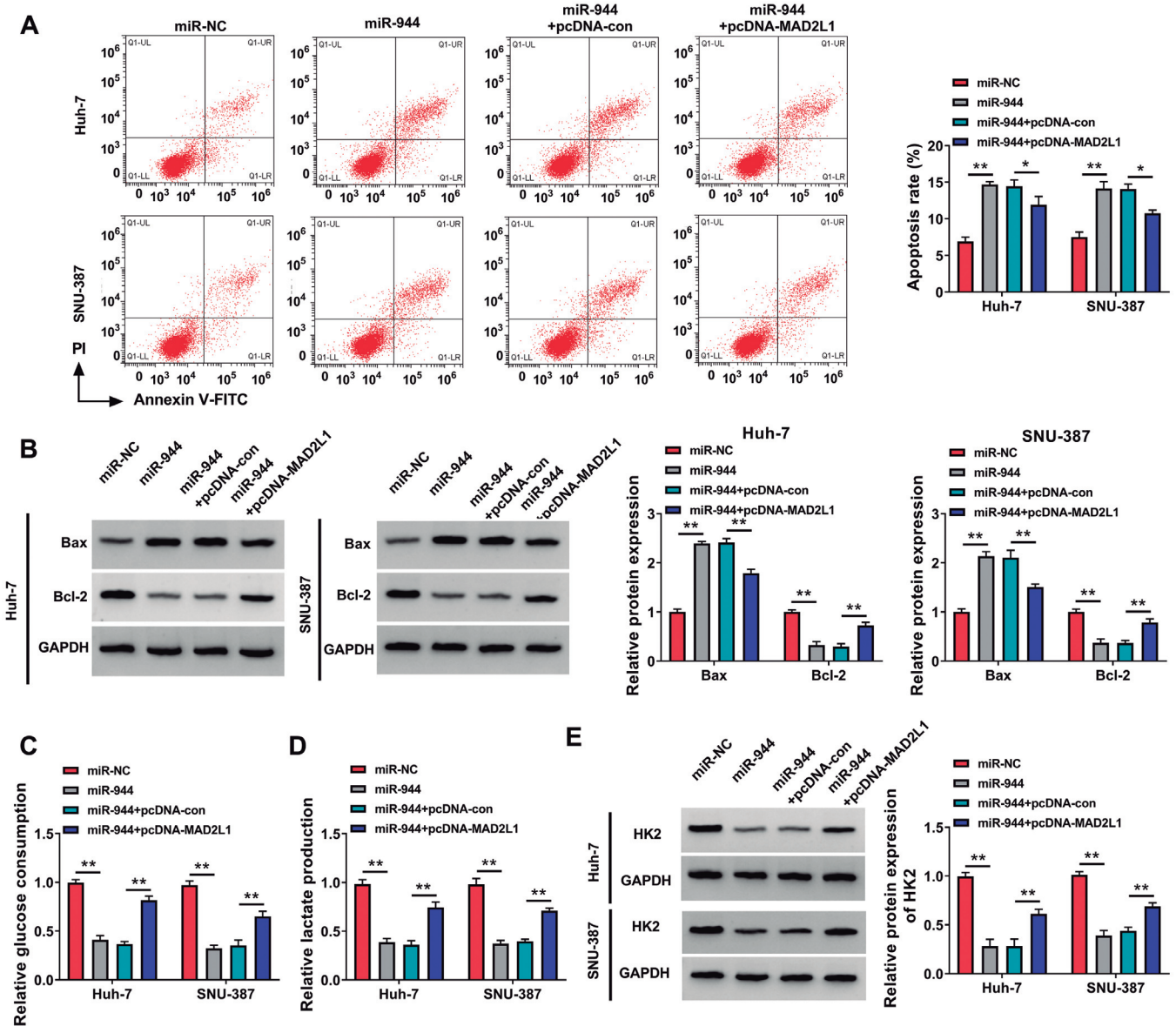

Fig. 9. Overexpression of MAD2L1 was able to rescue the suppression of high miR-944 expression on HCC cell progression. **A.** Apoptosis of transfected cells was gauged by flow cytometry. Bax and Bcl-2 protein expression **(B)**, glucose consumption **(C)**, lactate production **(D)**, and HK expression **(E)** were evaluated in SNU-387 and Huh-7 cells introduced by miR-944+pcDNA-MAD2L1, miR-944+pcDNA-con, miR-944 or miR-NC. *p<0.05, **p<0.01.

expression of Huh-7 and SNU-387 HCC cells (Fig. 8B). Strikingly, overexpression of miR-944 inhibited cell proliferation, which was weakened by MAD2L1 elevation (Fig. 8C-E). Moreover, the elevation of MAD2L1 enhanced cell migration and invasion, which were impeded by miR-944 overexpression in SNU-387 and Huh-7 cells (Fig. 8F,G). Also, MAD2L1 restoration reversed the influences of high miR-944 expression on cell apoptosis and the protein expression of Bax and Bcl-2 (Fig. 9A,B). Additionally, overexpression of MAD2L1 enhanced glucose consumption, lactate production and HK2 protein level, which were inhibited by miR-944 mimic transfection in SNU-387 and Huh-7 cells (Fig. 9C-E).

circ_0031242 regulated the expression of MAD2L1 protein through miR-944

To elucidate the relationships of si-circ_0031242, miR-944 and MAD2L1, we used western blot to examine MAD2L1 level in Huh-7 and SNU-387 transfected with si-circ_0031242, si-NC, si-circ_0031242+anti-miR-NC and si-circ_0031242+anti-miR-944. Expectedly, depletion of circ_0031242 reduced the level of MAD2L1 protein, which was reversed by inhibiting miR-944 expression in SNU-387 and Huh-7 HCC cells (Fig. 10A,B). Thus, circ_0031242 regulated MAD2L1 through miR-944.

Depletion of circ_0031242 inhibited HCC tumor growth

To further verify the effect of circ_0031242 on tumor growth, we injected Huh-7 cells transfected with sh-NC and sh-circ_0031242 into nude mice. By contrast, the tumor volume and weight were significantly reduced in the sh-circ_0031242 group (Fig. 11A-C). Moreover, circ_0031242 expression and MAD2L1 protein level were markedly lower in the sh-circ_003142 group compared with the control group, while miR-944 expression was enhanced in the sh-circ_0031242 tumor (Fig. 11D,E). IHC analysis showed that inhibition of circ_0031242 reduced cell staining with Ki67 in tumors (Fig. 11F). Thus, depletion of circ_003142 was able to inhibit tumor growth.

Discussion

High morbidity of HCC is one of the salient features in the world (Blum, 2011; Shen et al., 2018) Because only a fraction of the molecular mechanisms of HCC has been explored, understanding the precise actions of circRNAs in HCC remains limited.

CircRNAs have been discovered to be closely related to tumor growth and metastasis, including HCC (Qiu et al., 2019; Wang et al., 2020). For example, circANF566 contributed to cell progression in HCC by modulating the miR-4738-3p/TDO2 axis (Li et al., 2020b). Emerging evidence has ascertained that circ_0031242, produced by back-spliced exons 3-5 of the PRMT5 mRNA, is an essential regulatory factor in cancers, including esophageal cancer, breast cancer, gastric cancer, hepatoma, and non-small cell lung cancer (Du et al., 2019; Wang et al., 2019a-d; Ding et al., 2020a,b; Zhang et al., 2020; Wu et al., 2021). Consistent with previous research (Ding et al., 2020b), we demonstrated that circ_0031242 was upregulated in HCC, and knocking down circ_0031242 impeded HCC cell malignant behaviors.

MiRNAs are a family of key regulatory factors in cancers (Dou et al., 2016; Feng et al., 2017; Hong, 2017). Several reports have highlighted that miR-944 participates in cancer cell invasion and migration to mediate inflammation and tumorigenesis in cancers (Ji et al., 2018; An et al., 2019; Kim et al., 2019). Moreover, miR-944 is associated with chemoresistance and prognosis in cancers, implying that miR-944 was an

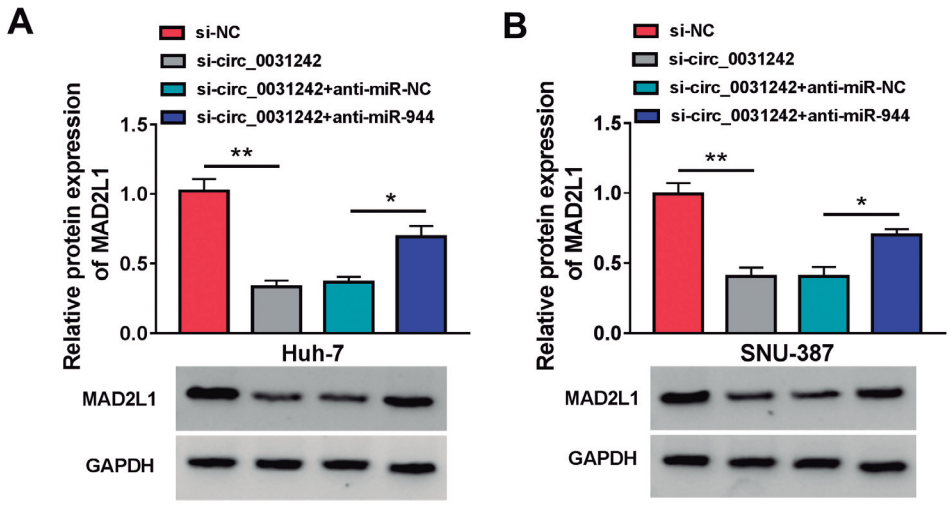

Fig. 10. Si-circ_0031242 inhibited the protein expression of MAD2L1 through regulating miR-944. **A and B.** MAD2L1 protein expression in Huh-7 and SNU-387 cells introduced by si-circ_0031242+anti-miR-944, si-circ_0031242+anti-miR-NC, si-NC, or si-circ_0031242. *p<0.05, *p<0.01.

indispensable factor in the regulatory mechanism of tumor formation and development (He et al., 2017; Peng et al., 2020). Here, we ascertained that circ_0031242 targeted miR-944 and, importantly, we uncovered that circ_0031242 affected cell progression of HCC through miR-944.

Accumulating evidence has shown that MAD2L1 might participate in the regulation of cell proliferation, invasion, and migration in various cancers (Foijer et al., 2017; Lu et al., 2020). Furthermore, MAD2L1, which acts as a target of miRNA, is involved in the regulatory network in tumorigenesis (Li et al., 2017; 2020a; Wang et al., 2019a-d). In this report, we illuminated that miR-944 participated in the cell growth of HCC through targeting MAD2L1. Moreover, circ_0031242 induced MAD2L1 through sponging miR-944. Animal experiments proved that suppression of circ_0031242 weakened tumorigenesis of HCC *in vivo*. Thus, the circ_003124/MIR-944/MAD2L1 axis was an important regulatory mechanism for HCC pathogenesis.

Conclusion

In summary, we established a new regulatory

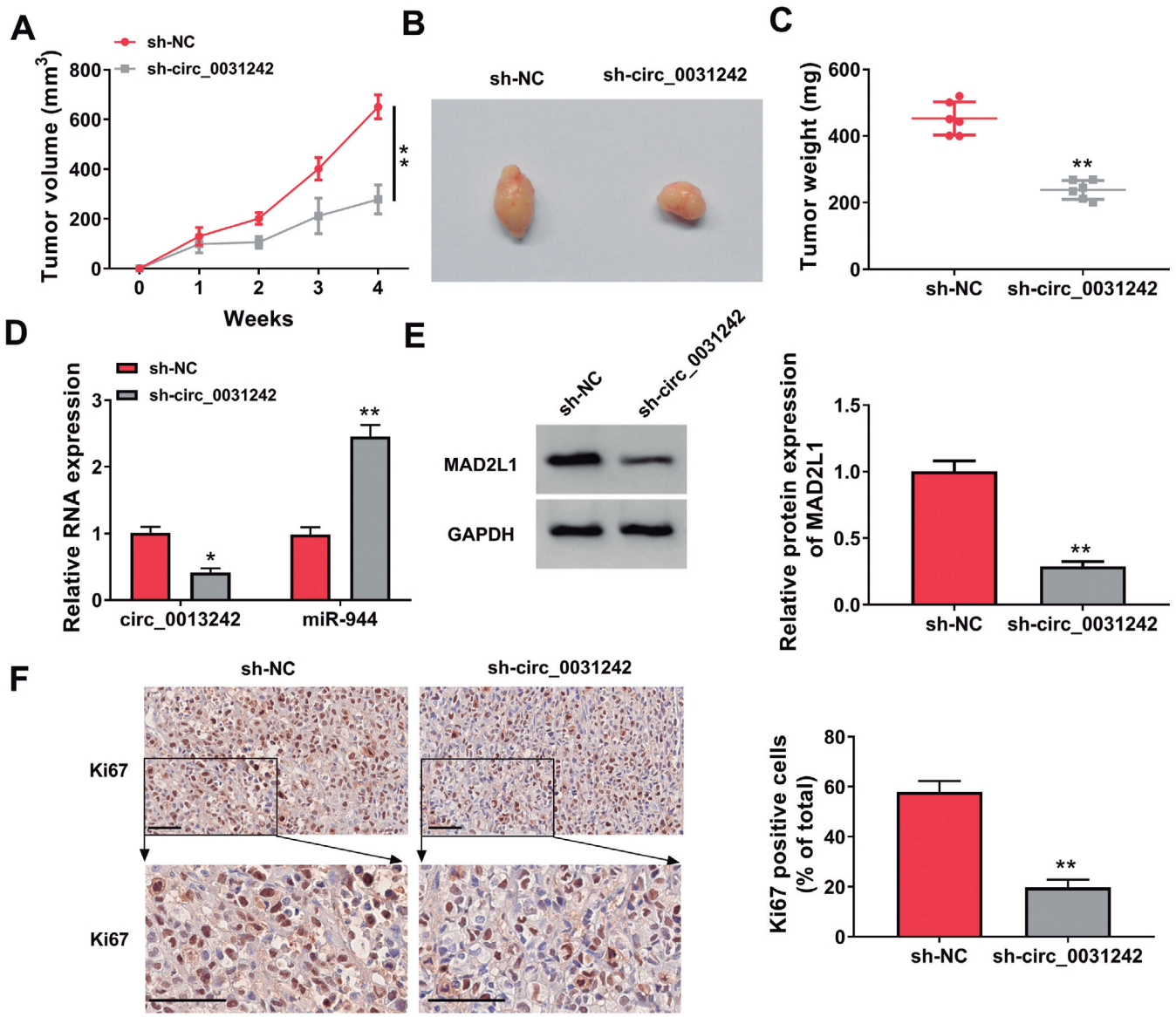

Fig. 11. Silencing of circ_003142 inhibited HCC tumor growth. **A-C.** The growth curves and weight of tumors. **D.** The expression of circ_0013242 and mR-944 was detected in sh-NC or sh-circ_0031242 groups in mice. **E.** The protein expression of MAD2L1 was measured in sh-NC or sh-circ_0031242 groups in mice. **F.** IHC analysis of Ki67 expression in sh-NC or sh-circ_0031242 groups in mice. *p<0.05, **p<0.01.

network for HCC. Circ_0031242 affected cell functional properties of HCC, providing a novel insight for HCC treatment.

Acknowledgements. Not applicable.

Ethics approval and consent to participate. The present study was approved by the ethical review committee of The First Affiliated Hospital of Shantou University Medical College. Written informed consent was obtained from all enrolled patients.

Consent for publication. Patients agreed to participate in this work.

Availability of data and materials. The analyzed data sets generated during the present study are available from the corresponding author on reasonable request.

Competing interests. The authors declare that they have no competing interests.

Funding. This work was supported by a grant from the Science and Technique Programs of Shantou City (NO.180404094011033).

References

An J.C., Shi H.B., Hao W.B., Zhu K. and Ma B. (2019). miR-944 inhibits lung adenocarcinoma tumorigenesis by targeting STAT1 interaction. Oncol. Lett. 17, 3790-3798.

Blum H.E. (2011). Hepatocellular carcinoma: HCC. Hepat. Mon. 11, 69-70.

Ding Z., Guo L., Deng Z. and Li P. (2020a). Circ-PRMT5 enhances the proliferation, migration and glycolysis of hepatoma cells by targeting miR-188-5p/HK2 axis. Ann. Hepatol. 19, 269-279.

Ding B., Fan W. and Lou W. (2020b). hsa_circ_0001955 enhances *in vitro* proliferation, migration, and invasion of HCC Cells through miR-145-5p/NRAS axis. Mol. Ther. Nucleic. Acids 22, 445-455.

Dou C., Liu Z., Xu M., Jia Y., Wang Y., Li Q., Yang W., Zheng X., Tu K. and Liu Q. (2016). miR-187-3p inhibits the metastasis and epithelial-mesenchymal transition of hepatocellular carcinoma by targeting S100A4. Cancer Lett. 381, 380-390.

Du W., Li D., Guo X., Li P., Li X., Tong S., Kuang L. and Liang D. (2019). Circ-PRMT5 promotes gastric cancer progression by sponging miR-145 and miR-1304 to upregulate MYC. Artif. Cells Nanomed. Biotechnol. 47, 4120-4130.

Feng Y., Yang C., Hu D., Wang X. and Liu X. (2017). miR-675 promotes disease progression of non-small cell lung cancer via activating NF-κB signaling pathway. Cell. Mol. Biol. 63, 7-10.

Foijer F., Albacker L.A., Bakker B., Spierings D.C., Yue Y., Xie S.Z., Davis S., Lutum-Jehle A., Takemoto D., Hare B., Furey B., Bronson R.T., Lansdorp P.M., Bradley A. and Peter K Sorger P.K. (2017). Deletion of the MAD2L1 spindle assembly checkpoint gene is tolerated in mouse models of acute T-cell lymphoma and hepatocellular carcinoma. Elife 6, 320873.

He Z., Xu H., Meng Y. and Kuang Y. (2017). miR-944 acts as a prognostic marker and promotes the tumor progression in endometrial cancer. Biomed. Pharmacother. 88, 902-910.

Hong L., Yang Z., Ma J. and Fan D. (2013). Function of miRNA in controlling drug resistance of human cancers. Curr. Drug Targets 14, 1118-1127.

Hsiao K.Y., Lin Y.C., Gupta S.K., Chang N., Yen L., Sun H.S. and Tsai S.J. (2017). Noncoding effects of circular RNA CCDC66 promote colon cancer growth and metastasis. Cancer Res. 77, 2339-2350.

Ji J., Peng Y., Niu T., Lin Y., Lin Y., Li X., Wu X., Huang Z., Zhong L. and Zhang S. (2018). miR-944 inhibits cell migration and invasion by targeting MACC1 in nasopharyngeal carcinoma. Int. J. Clin. Exp. Pathol. 11, 1167-1174.

Kaibori M., Yoshii K., Hasegawa K., Ogawa A., Kubo S., Tateishi R., Izumi N., Kadoya M., Kudo M., Kumada T., Sakamoto M., Nakashima O., Matsuyama Y., Takayama T., Kokudo N. and Liver Cancer Study Group of Japan (2019). Treatment optimization for hepatocellular carcinoma in elderly patients in a japanese nationwide cohort. Ann. Surg. 270, 121-130.

Kim Y.J., Lee J.H., Jin S., Kim J.H. and Kim S.H. (2019). Primate-specific miR-944 activates p53-dependent tumor suppression in human colorectal cancers. Cancer Lett. 440-441, 168-179.

Li Y., Bai W. and Zhang J. (2017). MiR-200c-5p suppresses proliferation and metastasis of human hepatocellular carcinoma (HCC) via suppressing MAD2L1. Biomed. Pharmacother. 92, 1038-1044.

Li J., He X., Wu X., Liu X., Huang Y. and Gong Y. (2020a). miR-139-5p inhibits lung adenocarcinoma cell proliferation, migration, and invasion by targeting MAD2L1. Comput. Math. Methods Med. 2020, 2953598.

Li S., Weng J., Song F., Li L., Xiao C., Yang W. and Xu J. (2020b). Circular RNA circZNF566 promotes hepatocellular carcinoma progression by sponging miR-4738-3p and regulating TDO2 expression. Cell Death Dis. 11, 452.

Lu S., Sun C., Chen H., Zhang C., Li W., Wu L., Zhu J., Sun F., Huang J., Wang J., Zhen Z., Cai R., Sun X., Zhang Y. and Zhang X. (2020). Bioinformatics analysis and validation identify CDK1 and MAD2L1 as prognostic markers of rhabdomyosarcoma. Cancer Manag. Res. 12, 12123-12136.

Peng H.Y., Hsiao J.R., Chou S.T., Hsu Y.M., Wu G.H., Shieh Y.S. and Shiah S.G. (2020). MiR-944/CISH mediated inflammation via STAT3 is involved in oral cancer malignance by cigarette smoking. Neoplasia 22, 554-565.

Qin M., Liu G., Huo X., Tao X., Sun X., Ge Z., Yang J., Fan J., Liu L. and Qin W. (2016). Hsa_circ_0001649: A circular RNA and potential novel biomarker for hepatocellular carcinoma. Cancer Biomark. 16, 161-169.

Qiu L., Wang T., Ge Q., Xu H., Wu Y., Tang Q. and Chen K. (2019). Circular RNA signature in hepatocellular carcinoma. J. Cancer 10, 3361-3372.

Qu Y., Dou P., Hu M., Xu J., Xia W. and Sun H. (2019). circRNA-CER mediates malignant progression of breast cancer through targeting the miR-136/MMP13 axis. Mol. Med. Rep. 19, 3314-3320.

Sang Y., Chen B., Song X., Li Y., Liang Y., Han D., Zhang N., Zhang H., Liu Y., Chen T., Li C., Wang L., Zhao W. and Yang Q. (2019). circRNA_0025202 regulates tamoxifen sensitivity and tumor progression via regulating the miR-182-5p/FOXO3a axis in breast cancer. Mol. Ther. 27, 1638-1652.

Shen X., Ma S., Tang X., Wang T., Qi X., Chi J., Wang Z., Cui D., Zhang Y. Li P. and Zhai B. (2018). Clinical outcome in elderly Chinese patients with primary hepatocellular carcinoma treated with percutaneous microwave coagulation therapy (PMCT): A Strobe-compliant observational study. Medicine (Baltimore) 97, e11618.

Wang X., Wang X., Li W., Zhang Q., Chen J. and Chen T. (2019a). Up-Regulation of hsa_circ_0000517 predicts adverse prognosis of hepatocellular carcinoma. Front. Oncol. 9, 1105.

Wang Y.G., Wang T., Ding M., Xiang S.H., Shi M. and Zhai B. (2019b). hsa_circ_0091570 acts as a ceRNA to suppress hepatocellular cancer progression by sponging hsa-miR-1307. Cancer Lett. 460, 128-138.

Wang Y., Li Y., He H. and Wang F. (2019c). Circular RNA circ-PRMT5 facilitates non-small cell lung cancer proliferation through upregulating EZH2 via sponging miR-377/382/498. Gene 720, 144099.

Wang Y., Wang F., He J., Du J., Zhang H., Shi H., Chen Y., Wei Y., Xue W., Yan J., Feng Y., Gao Y., Li D., Han J. and Zhang J. (2019d). miR-30a-3p targets MAD2L1 and regulates proliferation of gastric cancer cells. Onco. Targets Ther. 12, 11313-11324.

Wang F., Xu X., Zhang N. and Chen Z. (2020). Identification and integrated analysis of hepatocellular carcinoma-related circular RNA signature. Ann. Transl. Med. 8, 294.

Wei X., Zheng W., Tian P., He Y., Liu H., Peng M., Li X. and Liu X. (2020a). Oncogenic hsa_circ_0091581 promotes the malignancy of HCC cell through blocking miR-526b from degrading c-MYC mRNA. Cell Cycle 19, 817-824.

Wei Y., Chen X., Liang C., Ling Y., Yang X., Ye X., Zhang H., Yang P., Cui X., Ren Y., Xin X., Li H., Wang R., Wang W., Jiang F., Liu S., Ding J., Zhang B., Li L. and Wang H. (2020b). A noncoding regulatory RNAs network driven by Circ-CDYL acts specifically in the early stages hepatocellular carcinoma. Hepatology 71, 130-147.

Wu D., Jia H., Zhang Z. and Li S. (2021). Circ-PRMT5 promotes breast cancer by the miR-509-3p/TCF7L2 axis activating the PI3K/AKT pathway. J. Gene Med. 23, e3300.

Xiong D.D., Dang Y.W., Lin P., Wen D.Y., He R.Q., Luo D.Z., Feng Z.B. and Chen G. (2018). A circRNA-miRNA-mRNA network identification for exploring underlying pathogenesis and therapy strategy of hepatocellular carcinoma. J. Transl. Med. 16, 220.

Yao J.T., Zhao S.H., Liu Q.P., Lv M.Q., Zhou D.X., Liao Z.J. and Nan K.J. (2017). Over-expression of CircRNA_100876 in non-small cell lung cancer and its prognostic value. Pathol. Res. Pract. 213, 453-456.

Yao Z., Xu R., Yuan L., Xu M., Zhuang H., Li Y., Zhang Y. and Lin N. (2019). Circ_0001955 facilitates hepatocellular carcinoma (HCC) tumorigenesis by sponging miR-516a-5p to release TRAF6 and MAPK11. Cell Death Dis. 10, 945.

Zhang Y., Liu H., Li W., Yu J., Li J., Shen Z., Ye G., Qi X. and Li G. (2017). CircRNA_100269 is downregulated in gastric cancer and suppresses tumor cell growth by targeting miR-630. Aging (Albany NY) 9, 1585-1594.

Zhang X., Xu Y., Qian Z., Zheng W., Wu Q., Chen Y., Zhu G., Liu Y., Bian Z., Xu W., Zhang Y., Sun F., Pan Q., Wang J., Du L. and Yu Y. (2018). circRNA_104075 stimulates YAP-dependent tumorigenesis through the regulation of HNF4a and may serve as a diagnostic marker in hepatocellular carcinoma. Cell Death Dis. 9, 1091.

Zhang L.W., Wang B., Yang J.X. and Yang H. (2020). Circ-PRMT5 stimulates migration in esophageal cancer by binding miR-203. Eur. Rev. Med. Pharmacol. Sci. 24, 9965-9972.

Accepted September 20, 2022